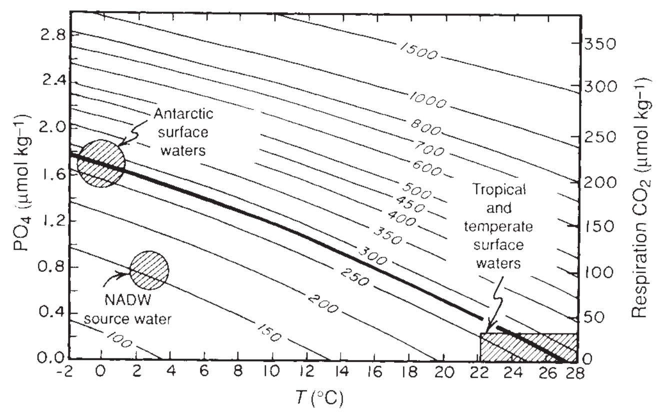

FIG. 3 Contours of CO_2 partial pressure (in μatm) for a water sample with a salinity of 35‰, a respiration free $\sum CO_2$ concentration of 1,900 μmol kg^{-1} and an alkalinity of 2,310 μequiv kg^{-1} as a function of water temperature and phosphate content (and hence also respiration CO_2 content). We assume a C/P ratio of 127 and a N/P ratio of 16 for the marine organic matter oxidized within the sea. The heavy contour is that representing the pre-industrial atmosphere (280 μatm). Note that in the real ocean, fresh-water-induced salinity and $CaCO_3$-induced alkalinity differences create additional texture in the distribution of CO_2 partial pressure in surface water. The important point here is that the high content of respiration CO_2 compensates for the low temperature of Antarctic surface waters, giving them nearly the same CO_2 partial pressure as warm nutrient-free surface water. By contrast, because of their lower respiration CO_2 content, surface waters in the northern Atlantic have much lower CO_2 pressures. As a consequence, surface waters in the northern Atlantic take up CO_2 given off to the atmosphere by other regions of the ocean.

enough to compensate for their lower temperature. By contrast, because of their lower content of respiration CO_2, surface waters in the northern Atlantic have a strong tendency to take up CO_2 from the atmosphere. Thus it is the difference in respiration CO_2 content which creates the tendency to pump CO_2 through the ocean from north to south and through the atmosphere from south to north.

Our estimate of 0.6 gigatonnes for the natural transport of carbon through the ocean from the Northern to the Southern Hemisphere can be compared with that of 0.26 gigatonnes obtained by Brewer *et al.*[12] for the net southward transport across a section at 25° N in the Atlantic. As Brewer *et al.* did not correct for fossil-fuel CO_2 carried northward by the upper waters, their estimate provides only the lower limit on the pre-industrial interhemispheric transport.

According to our calculations, transport of excess CO_2 by the Atlantic's conveyor accounts for ~60% of the mismatch between the amount of CO_2 currently being transported across the Equator and the amount required to explain the increases observed for the Southern Hemisphere atmosphere and calculated for the Southern Hemisphere ocean. The 0.6 gigatonnes of CO_2 naturally released from the southern ocean offsets part but not all of the one gigatonne uptake of anthropogenic CO_2 calculated by oceanographers. Thus, although it does not invalidate the case made by Tans *et al.*[3] for a reduced CO_2 uptake by the ocean and an increased CO_2 uptake by the north temperate terrestrial biosphere, our finding removes much of the punch of this argument. It also lends support to the proposal by Keeling and Heimann[1,2] that a south-to-north decrease in atmospheric CO_2 content existed before the Industrial Revolution. The challenge will be to document this small difference directly through ultra-precise measurements of CO_2 to air ratios in pre-industrial ice from Antarctica and from Greenland. □

Received 3 December 1991; accepted 24 February 1992.

1. Heimann, M. & Keeling, C. D. *J. geophys. Res.* **91,** 7765–7781 (1986).
2. Keeling, C. D. & Heimann, M. *J. geophys. Res.* **91,** 7782–7796 (1986).
3. Tans, P. P., Fung, I. Y. & Takahashi, T. *Science* **247,** 1431–1438 (1990).
4. Broecker, W. S. *Oceanography* **4,** 79–89 (1991).
5. Broecker, W. S., Virgilio, A. & Peng, T.-H. *Geophys. Res. Lett.* **18,** 1–3 (1991).
6. Takahashi, T., Broecker, W. S. & Langer, S. *J. geophys. Res.* **90,** 6907–6924 (1985).
7. Broecker, W. S., Takahashi, T. & Takahashi, T. T. *J. geophys. Res.* **90,** 6925–6939 (1985).
8. Peng, T.-H. & Broecker, W. S. *Global biogeochem. Cycles* **1,** 155–161 (1987).
9. Broecker, W. S. *et al. Global biogeochem. Cycles* **5,** 87–117 (1991).
10. Dickson, R. R., Gmitrowicz, E. M. & Watson, A. J. *Nature* **344,** 848–850 (1990).
11. Bryden, H. L. & Hall, M. M. *Science* **207,** 884–886 (1980).
12. Brewer, P. G., Goyet, C. & Dyrssen, D. *Science* **246,** 477–479 (1989).
13. Bainbridge, A. E. *GEOSECS Atlantic Ocean Expedition Hydrographic Data VI* (NSF, Washington DC, 1981).
14. Broecker, W. S., Spencer, D. W. & Craig, H. *GEOSECS Pacific Ocean Expedition Hydrographic Data V3* (NSF, Washington DC 1982).
15. Weiss, R. F. *et al. GEOSECS Indian Ocean Expedition Hydrographic Data V5* (NSF, Washington DC, 1983).
16. *Transient Tracers in the Ocean, North Atlantic Study, Shipboard Phys. chem. Data Rep.* (Scripps Institution of Oceanography, San Diego, 1986).
17. *CSS Hudson Cruise 82-001, Vol. 1, Phys. chem. Data Rep.* (Scripps Institution of Oceanography, San Diego, 1984).
18. *Transient Tracers in the Ocean, Tropical Atlantic Study, Shipboard Phys. chem. Data Rep.* (Scripps Institution of Oceanography, San Diego, 1986).
19. *South Atlantic Ventilation Experiment, Preliminary Shipboard Chem. Phys. Data Rep.* (Legs 1–5) (Scripps Institution of Oceanography, San Diego, 1988–1989).

ACKNOWLEDGEMENTS. We thank M. Heimann and E. Maier-Reimer for help, and T. Takahashi for supplying compatible $\sum CO_2$ data sets for the TTO, TAS and SAVE expeditions. This work is supported by the US Department of Energy CO_2 Program (W.S.B.) and Martin Marietta Energy Systems, Inc. (T.T.P.).

Revised budget for the oceanic uptake of anthropogenic carbon dioxide

J. L. Sarmiento* & E. T. Sundquist†

* Atmospheric and Oceanic Sciences Program, Princeton University, Princeton, New Jersey 08544-0710, USA
† United States Geological Survey, Woods Hole, Massachusetts 02543, USA

TRACER-CALIBRATED models of the total uptake of anthropogenic CO_2 by the world's oceans give estimates of about 2 gigatonnes carbon per year[1], significantly larger than a recent estimate[2] of 0.3–0.8 Gt C yr^{-1} for the synoptic air-to-sea CO_2 influx. Although both estimates require that the global CO_2 budget must be balanced by a large unknown terrestrial sink, the latter estimate implies a much larger terrestrial sink, and challenges the ocean model calculations on which previous CO_2 budgets were based. The discrepancy is due in part to the net flux of carbon to the ocean by rivers and rain, which must be added to the synoptic air-to-sea CO_2 flux to obtain the total oceanic uptake of anthropogenic CO_2. Here we estimate the magnitude of this correction and of several other recently proposed adjustments to the synoptic air–sea CO_2 exchange. These combined adjustments minimize the apparent inconsistency, and restore estimates of the terrestrial sink to values implied by the modelled oceanic uptake.

Table 1*a* shows annual anthropogenic CO_2 budgets for recent years as summarized by the Intergovernmental Panel on Climate Change (IPCC)[1] and Tans *et al.*[2]. Both budgets show large imbalances which are generally attributed to uptake by terrestrial vegetation and/or soils[3], although firm evidence for this uptake is difficult to obtain and the uncertainties are therefore large. The IPCC budget was based on models of ocean CO_2 uptake which imply a net terrestrial carbon flux near zero (Table 1*b*). Tans *et al.* estimated the synoptic air-to-sea CO_2 flux by combining the results of an atmospheric transport model with a compilation of observations of air–sea CO_2 difference. They concluded that the limited rate of atmospheric transport of anthropogenic CO_2 from the Northern Hemisphere restricts ocean CO_2 uptake south of the Equator, and the air–sea CO_2 observations set limits on oceanic CO_2 absorption in the Northern Hemisphere. They proposed that ocean CO_2 uptake constrained in this way must be 0.3–0.8 Gt C yr^{-1}, requiring a total net terrestrial uptake of ~1.5–2.0 Gt C yr^{-1} (Table 1*b*).

TABLE 1 Budgets for anthropogenic perturbation of CO_2

(*a*) IPCC[1] and Tans *et al.*[2]

	Average perturbation (Gt C yr^{-1})	
	IPCC*	Tans *et al.*†
Sources		
Fossil	5.4 ± 0.5	5.3
Deforestation	1.6 ± 1.0	0.0–3.2
Total	7.0 ± 1.2	5.3–8.5
Sinks		
Atmosphere	3.2 ± 0.1	3.0
Oceans (steady-state models)	2.0 ± 0.8	0.3–0.8
Total	5.2 ± 0.8	3.3–3.8
Imbalance (inferred terrestrial uptake)	1.8 ± 0.4	2.0–4.7

(*b*) Comparison of the IPCC terrestrial and oceanic sinks[1] with the budget of Tans *et al.*[2]

	IPCC*	Tans *et al.*†
(1) Inferred terrestrial uptake	1.8 ± 1.4	2.0–4.7
(2) Deforestation	1.6 ± 1.0	0.0–3.2
Net terrestrial uptake, (1) − (2)	0.2 ± 1.7	1.5–2.0
Net ocean uptake	2.0 ± 0.8	0.3–0.8
Total uptake (terrestrial + ocean)	2.2 ± 1.9	2.3

(*c*) Modified IPCC[1] and Tans *et al.*[2] ocean sink budgets

	Fluxes in Gt C yr^{-1}
Revised Tans *et al.* budget	
Tans *et al.* synoptic estimates of air–sea input	0.3–0.8
Correction for skin temperature effect	0.1–0.6
Correction for carbon monoxide budget	0.3
Modified estimate of air–sea input	0.7–1.7
Net river inorganic carbon flux	0.2–0.3
Net river organic carbon flux	0.2–0.4
Total ocean uptake	1.1–2.4
Revised IPCC budget	
Model estimates of oceanic uptake	1.7–2.8

* The IPCC budget covers the period 1980–89. The atmospheric sink has been reduced to 3.2 ± 0.1 from the original IPCC value 3.4 ± 0.2 (P. Tans, personal communication).

† The Tans *et al.* budget is based on their scenarios 5–8, which make use of an atmospheric transport model constrained by the interhemispheric gradient of CO_2 as estimated from observations for the period 1980–87, and by oceanic observations in the region between 15° S and 90° N for the period 1972–89. The 15° S–90° N oceanic observations give a global uptake of 0.35 Gt C yr^{-1} with the gas exchange coefficient of ref. 9, and 0.71 Gt C yr^{-1} with an empirical gas exchange coefficient based on observations of ocean uptake of bomb radiocarbon. The Tans *et al.* scenarios adjust the Southern Hemisphere ocean uptake so that the total ocean uptake with the two different gas exchange coefficients is comparable. The total terrestrial and ocean uptake is fixed at 2.3 Gt C yr^{-1} in all their scenarios.

TABLE 2 Estimated marine and terrestrial pre-industrial carbon budgets

(*a*) Geochemical ocean inorganic carbon budget*

	Flux (Gt C yr^{-1})			
	Berner *et al.*[23]	Berner and Berner[24]	Meybeck[25]	Drever *et al.*[26]
(1) River dissolved inorganic carbon	0.429	0.390	0.439	0.385
(2) Marine carbonate sedimentation	0.221	0.204	0.236	0.127–0.170
(1) − (2)	0.208	0.186	0.203	0.215–0.258
Decarbonation	0.071	0.080	0.077	—
Implied ocean–atmosphere flux of CO_2	0.21–0.28	0.19–0.27	0.20–0.28	0.21–0.26

(*b*) Recent estimates of global river organic carbon fluxes

	Flux estimates (Gt C yr^{-1})		
Reference	Dissolved organic carbon	Particulate organic carbon	Total organic carbon
Schlesinger and Melack[27]	—	—	0.37
	—	—	0.41
Meybeck[28]	0.215	0.179	0.383
Milliman *et al.*[29]	—	(0.295)†	—
Ittekot[30]	—	0.231	—
Meybeck[31]	0.206	0.169	0.302 (0.375)‡
Spitzy and Leenheer[32]	0.22	—	—
Degens *et al.*[33]	—	—	0.33 (0.365)§
'Best' estimates	0.2	0.2–0.3	0.3–0.5‖

(*c*) Estimated terrestrial and marine organic carbon budgets

	Flux (Gt C yr^{-1})
Oceans	
Additions by rivers	0.3–0.5
Burial in sediments	−0.1
Net loss to CO_2	0.2–0.4
Land	
Production delivered to rivers	−0.3–−0.5
Net oxidation or organic carbon in rocks	0.1
Net production from CO_2	−0.2–−0.4

* The estimates of refs 23–25 are all based on the assumption of a steady state with stoichiometry similar to the reactions in Fig. 1*a* and *b*. A small correction was applied by the authors of these estimates to account for weathering by H_2SO_4 from pyrite oxidation on land, balanced by alkalinity production during sulphate reduction in marine sediments. These processes result in a bicarbonate river flux to the ocean, balanced by an equal amount of $CaCO_3$ burial in the sediments, and explain why row (2) is more than 50% of row (1). The estimates of ref. 26 were not constrained to a steady state and did not include an estimate of silicate weathering and decarbonation.

† Based on the revision suggested in ref. 29 of the particulate organic carbon flux estimates of Meybeck[28].

‡ Calculated as sum of dissolved organic carbon and particulate organic carbon fluxes; disagreement with the total organic flux estimate of ref. 31 is due to extrapolation from different data sets.

§ The estimate of ref. 33 for the total organic carbon flux for Asia is biased towards the relatively low ratios of total organic carbon to discharge measured in the rivers flowing into the Arctic Ocean. Using their total organic carbon data and method of extrapolation, but extrapolating separate estimates for northern and southern Asian rivers, we calculate an increase of 18% (from 0.169 to 0.200 Gt C yr^{-1}) in the aggregate extrapolated total organic carbon flux from Asia.

‖ The maximum estimate is calculated as the sum of the maximum 'best' estimates for dissolved organic carbon and particulate organic carbon.

Such a small oceanic sink for anthropogenic CO_2 is inconsistent with many ocean models. For example, the work of Sarmiento *et al.*[4], which makes use of a three-dimensional ocean model validated against bomb radiocarbon observations[5], gives an estimate of 1.9 Gt C yr^{-1} for the decade 1980–89 and 1.7 Gt C yr^{-1} for the period 1972–89, which is the time span of the data set used by Tans *et al.*[2]. Sarmiento *et al.* conclude that these estimates probably represent a lower limit; the ocean circulation model underestimates the bomb radiocarbon uptake because of factors that would also underestimate the uptake of anthropogenic CO_2. We therefore suggest 1.7 Gt C yr^{-1} as a lower limit for the modelled oceanic uptake of anthropogenic CO_2 while retaining the IPCC upper limit of 2.8 Gt C yr^{-1} (Table 1*c*).

Although the air–sea CO_2 flux estimates of ref. 2 are based on the most comprehensive available data set, they may not accurately represent average annual air–sea CO_2 differences. We doubt, however, that improved temporal and spatial resolution could account for a systematic Northern Hemisphere flux error in excess of 1 Gt C yr^{-1}, which would be required to reconcile the results of ref. 2 with the ocean model results. The difficulty can be illustrated by comparing air–sea CO_2 differences calculated by Tans *et al.* with those derived from a recent model study[6], which includes the interhemispheric transport constraint discussed by Tans *et al.*, but ignores the estimates of air-sea CO_2 flux in the Northern Hemisphere, using instead the uptake of 2.3 Gt C yr^{-1} estimated for 1984 from an oceanic model. This model requires an air-sea CO_2 difference of +19 p.p.m. in the Pacific north of 15.6° N, compared with an estimate of −2 p.p.m. based on the data of Tans *et al.*, and an air-sea difference of +52 p.p.m. north of 23.5° N in the Atlantic, compared with data-based estimates by Tans *et al.* of +37 p.p.m. north of 50° N and +15 p.p.m. between 15° and 50° N.

An important factor not accounted for by Tans *et al.*[2] is the observation that skin temperatures of water at the surface of the ocean are usually colder than the bulk temperatures normally used in determining air-sea pCO_2 differences. One recent study[7] in the North Atlantic showed that surface temperatures were ~0.11 °C colder than bulk temperatures at day, on average, and ~0.3 °C colder during the night.[7] The solubility of CO_2 in water increases by 3-4% per °C cooling, with the result that the cooler skin temperatures would give an increase in the average of data-based air-sea CO_2 difference estimates of ~1.1-4.3 p.p.m. (see, for example, Smethie *et al.*[8]). This correction could have a considerable effect on the global carbon budgets (A. Watson, personal communication). An increase of this magnitude in the air-sea CO_2 difference over the entire globe would give an increased flux of CO_2 into the ocean of 0.14-0.54 Gt C yr^{-1}, assuming a mean global gas exchange coefficient of 0.029 mol m^{-2} yr^{-1} per p.p.m. (ref. 9). An average gas exchange coefficient high enough to explain the bomb radiocarbon observations (this would be 0.061 mol m^{-2} yr^{-1} per p.p.m.; see ref. 5), would give an increase in the observationally based ocean uptake estimate of 0.29-1.12 Gt C yr^{-1}. Tans *et al.*[2] made use of ocean observations only for the region north of 15° S (57% of the ocean area), so the total range of these estimated corrections (0.14 to 1.12) would have to be multiplied by ~0.57, giving 0.1-0.6 Gt C yr^{-1}, to account for the skin temperature effect (Table 1*c*).

Another correction is for the effect of carbon monoxide transport and oxidation on the CO_2 budget. Carbon monoxide is produced mainly in the Northern Hemisphere by industrial and biotic processes[10]. It is oxidized to CO_2 primarily by reaction with hydroxyl in the atmosphere both north and south of the Equator. These sources and sinks effectively mediate the transport of 0.25-0.29 Gt C yr^{-1} of fossil-fuel CO_2 to the Southern Hemisphere as atmospheric carbon monoxide[11]. Tans *et al.* did not include this transfer in their calculations, although they did briefly mention it. We assume that the main sink for this carbon monoxide-mediated interhemispheric CO_2 transport is the Southern Hemisphere ocean, and include it as a correction to the Tans *et al.* oceanic uptake shown in Table 1*c*.

Geochemists have long postulated a net CO_2 flux associated with the river flux of carbon into the ocean. Its possible contribution to the anthropogenic CO_2 budget has been noted before (see, for example, ref. 12), but was not included in the oceanic uptake estimated in ref. 2, nor were its full implications noted in ref. 12 for the comparison between the Tans *et al.* budget and the ocean model estimates of anthropogenic CO_2 uptake. Even if there were no anthropogenic CO_2 source, the river carbon flux must be geochemically balanced by a small but important long-term net CO_2 flux from the oceans to the atmosphere.

The dominant geochemical fluxes affecting CO_2 are those

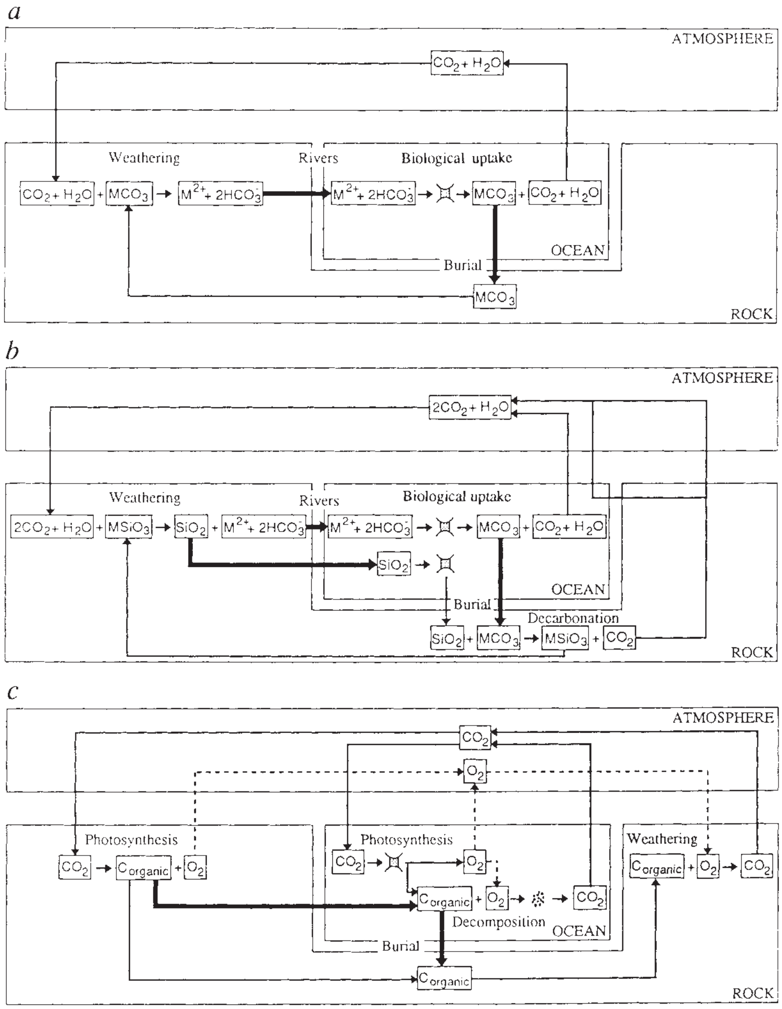

FIG. 1 Illustration of the effect of the carbonate, silicate and organic carbon budgets on air-sea exchange of CO_2. M symbolizes a generic cation such as Ca^{2+}. The thick arrows indicate the actual fluxes that are summarized in Table 2. *a*, Carbonate budget. The flux of bicarbonate into the ocean by rivers is balanced by a 50% loss of CO_2 to the atmosphere and a 50% loss of MCO_3 to the sediments. The ocean-to-atmosphere flux can be estimated from the river bicarbonate flux minus the sediment burial of MCO_3. *b*, Silicate budget. Again, this implies a CO_2 flux that can be estimated by subtracting the burial of MCO_3 from the river flux of bicarbonate, as in the carbonate budget. The volcanic and metamorphic decarbonation reaction releases additional CO_2 which must enter the amosphere to close the budget, and can do so either through the ocean or directly to the atmosphere. The decarbonation flux is estimated from the silicate weathering flux and is treated as an uncertainty, as discussed in the text. *c*, Organic carbon budget. This has two parts: the terrestrial burial and riverine export of photosynthetic carbon (left) requires a net terrestrial uptake of CO_2 which must be met by a flux out of the ocean; the oceanic burial of photosynthetic carbon must be balanced by a net oxidation on land (right), which results in CO_2 uptake by the ocean. At steady state, the net air-sea exchange of CO_2 must be balanced by all of these processes, among which the riverine organic flux predominates. One can therefore estimate the effect of the organic carbon budget on air-sea exchange from the river flux of organic carbon minus the ocean sediment burial of organic carbon.

TABLE 3 Spatial distribution of ocean to atmosphere CO_2 flux

Latitude band	*A* Revised Tans *et al.*[2] budget*	*B* Anthropogenic CO_2 uptake estimate†	$C=A-B$ Estimated pre-industrial fluxes
>15° N	−0.66	−0.38	−0.28
15° S–15° N	1.22	−0.48	+1.70
15° S–50° S	−2.15	−0.41	−1.74
>50° S	0.50	−0.42	+0.92
Total	−1.09	−1.69	+0.60

* The Tans *et al.*[2] budget is based on their scenario 6. This scenario gives an ocean uptake of −0.69 Gt C yr^{-1} which needs to be increased to −1.09 Gt C yr^{-1} to match the pre-industrial ocean efflux estimate of 0.6 Gt C yr^{-1} shown in column *C*, added to the anthropogenic CO_2 uptake estimate of column *B*. This is accomplished by adding the −0.25 Gt C yr^{-1} carbon monoxide correction obtained by Enting and Mansbridge[11] to the 15° S–50° S band, and by adding a further −0.15 Gt C yr^{-1} skin-temperature correction split evenly between the equal areas of the equatorial and Northern Hemisphere bands. The reason for putting all of the Southern Hemisphere carbon monoxide correction into the 15° S–50° S band instead of including part of it in the >50° S band is that Tans *et al.* use a fixed Southern Ocean efflux of 0.5 Gt C yr^{-1} in all their model scenarios. The skin-temperature correction is applied to the two latitude bands in which the Tans *et al.* estimate uses the air–sea exchange estimates obtained from measurements.

† The anthropogenic CO_2 uptake estimate is taken from the simulation of ref. 4 for the same time span (1972–89) as the data set of Tans *et al.*[2].

associated with carbonate weathering, silicate weathering, and organic carbon production and remineralization (Fig. 1). Because these fluxes are difficult to measure, they are usually approximated using steady-state assumptions. Such assumptions are questionable. For example, Wollast and Mackenzie[13] have suggested that anthropogenic effects may enhance CO_2 release into the ocean by as much as ~0.6 Gt C yr^{-1}. But because non-steady-state CO_2 will be buffered by reaction with the very large pool of dissolved inorganic carbon in the ocean, the actual flux of non-steady-state CO_2 from the ocean to the atmosphere will be only ~17% of that produced[4,14]. Even the pronounced effect proposed by Wollast and Mackenzie should only increase CO_2 evasion by ~0.1 Gt C yr^{-1}. Thus we believe that steady-state-based estimates are a reasonable representation of the present-day geochemical CO_2 budget.

For the combined carbonate and silicate geochemical cycles (Fig. 1*a*, *b*), the magnitude of the flux of CO_2 out of the ocean can be estimated as the difference between carbon entering the ocean as dissolved inorganic carbon (primarily HCO_3^-) in rivers, and the loss of carbon to the sediments as $CaCO_3$ (ref. 15). Table 2*a* summarizes recent estimates for these two quantities. To complete the geochemical steady state, a separate source of CO_2 is necessary to balance the CO_2 consumed during silicate weathering and subsequently buried in carbonate sediments (Fig. 1*b*). This source of CO_2 is thought to be the decarbonation of carbonate minerals during metamorphism and volcanism. The flux of CO_2 produced by decarbonation can enter the atmosphere either directly or through the ocean. Because the ocean component of the decarbonation flux is very uncertain[16], the total decarbonation flux is treated as an uncertainty in Table 2*a*. Given the uncertainties, we estimate that the carbonate and silicate geochemical cycles require an ocean-to-air CO_2 flux of ~0.2–0.3 Gt C yr^{-1}.

Like the carbonate and silicate cycles, the geochemical organic carbon cycle can be approximated as a steady state for the purpose of deriving preliminary estimates of the implied CO_2 flux. Perhaps the simplest steady-state approach is to assume that there is a flux of CO_2 out of the ocean equal to the organic carbon flux into the ocean by rivers, minus the burial of organic carbon in marine sediments[17]. From river flux estimates (Table 2*b*) we conclude that the most likely total organic carbon load in rivers globally is ~0.3–0.5 Gt C yr^{-1}. The burial of organic carbon in sediments has been estimated[17,18] at ~0.1 Gt C yr^{-1}, giving an implied CO_2 flux of 0.2–0.4 Gt C yr^{-1} that must be transferred from the oceans to the land by way of the atmosphere (Table 2*c*).

A considerable uncertainty affecting our hypothesis is the extent to which estuarine and continental shelf processes alter carbon transfer from rivers to the open ocean. The principal sink for riverine inorganic carbon is carbonate sedimentation, which occurs almost exclusively in waters removed from fresh water inputs. The distribution of dissolved organic carbon seems to be conservative in many estuaries[19]. The fate of particulate organic carbon in estuaries is more complex. Although some riverine organic carbon may not be transported through estuaries, additional terrestrial organic carbon may reach the oceans by transport in marine aerosols[20]. The average air–sea CO_2 difference that would be required in shelf regions (7.5% of the ocean area) to release the entire geochemical CO_2 flux is ~20–74 p.p.m., assuming the range of global average gas-exchange coefficients given above. Because the equilibration time of ocean surface water with respect to CO_2 gas exchange is about one year[21], it seems unlikely to us that the shelf regions could maintain such large global average air–sea differences without significantly affecting the open ocean. More data from coastal regions are needed, but those that are available suggest that CO_2 exchange in shelf regions is related primarily to large-scale oceanic features (such as upwelling zones) rather than local river fluxes.

We therefore conclude that the ocean CO_2 budget must be offset by ~0.4–0.7 Gt C to account for the steady-state geochemical fluxes (Table 1*c*). When combined with adjustments for the skin-temperature and carbon monoxide corrections, these fluxes bring the CO_2 budget of Tans *et al.*[2] to within a range that overlaps that of the revised IPCC budget[1], without requiring that the ocean models be incorrect, or that the air–sea CO_2 measurements be biased. We therefore believe that the summary given in Table 1*c* supports the overall conclusion that there is essentially no conflict between the estimates of uptake from ocean models and the observationally based estimates of Tans *et al.*[2].

It will not be easy to constrain the estimates of river carbon transport further, or to determine the latitudinal distribution of the associated CO_2 fluxes. Limited oceanic uptake of CO_2 in the Southern Hemisphere implies that a large fraction of the geochemical CO_2 efflux must effectively be leaving the ocean there (Table 3). Such an efflux may be maintained by interhemispheric southward flow of North Atlantic Deep Water[22]. Additional observations can be done to constrain the skin-temperature correction as well as the poorly known contribution of estuaries and shelf regions to the oceanic carbon budget. The results of Keeling *et al.*[6] suggest that the distribution of ^{13}C in the atmosphere is not consistent with the large terrestrial vegetation sink postulated by Tans *et al.*[2]. The geochemical flux and other corrections we postulate similarly reduce the inferred terrestrial sink for anthropogenic CO_2 to a magnitude consistent with the models of ocean CO_2 uptake. Additional terrestrial carbon uptake is required, however, to supply the geochemical river fluxes (Table 1*c*). Future analysis of the atmospheric ^{13}C distribution may provide important further constraints. □

Received 15 October 1991; accepted 24 March 1992.

1. Houghton, J. T., Jenkins, G. J. & Ephraums, J. J. *Climate Change, The IPCC Scientific Assessment* (Cambridge University Press, 1990).
2. Tans, P. P., Fung, I. Y. & Takahashi, T. *Science* **247**, 1431–1438 (1990).
3. Siegenthaler, U. & Oeschger, H. *Tellus* B39, 140–154 (1987).
4. Sarmiento, J. L., Siegenthaler, U. & Orr, J. C. *J. geophys. Res.* **97**, 3621–3645 (1992).
5. Toggweiler, J. R., Dixon, K. & Bryan, K. *J. geophys. Res.* **94**, 8243–8264 (1989).
6. Keeling, C. D., Piper, S. C. & Heimann, M. in *Aspects of Climate Variability in the Pacific and the Western Americas, Geophys. Monogr.* 55 (ed. Peterson, D. H.) 305–363 (American Geophysical Union, Washington DC, 1989).

7. Schluessel, P., Emery, W. J., Grassl, H. & Mammen, T. *J. geophys. Res.* **95**, 13341–13356 (1990).
8. Smethie, W. M. Jr., Takahashi, T. & Chipman, D. W. *J. geophys. Res.* **90**, 7007–7022 (1985)
9. Liss, P. & Merlivat, L. in *The Role of Air–Sea Exchange in Geochemical Cycling* (ed. Buat-Menard, P.) 113–127 (Reidel, Dordrecht, 1986).
10. Crutzen, P. J. & Gidel, L. T. *J. geophys. Res.* **88**, 6641–6661 (1983).
11. Enting, I. G. & Mansbridge, J. V. *Tellus* **B43**, 156–170 (1991).
12. Sabine, C. L. & Mackenzie, F. T. *Int. J. Energy Envir. Econ.* **1**, 119–127 (1991).
13. Wollast, R. & Mackenzie, F. T. *Climate and Geosciences: A Challenge for Science and Society in the 21st Century*, 453–473 (Kluwer, Dordrecht, 1989).
14. Maier-Reimer, E. & Hasslemann, K. *Clim. Dynam.* **2**, 63–90 (1987).
15. Mackenzie, F. T. & Garrels, R. M. *Am. J. Sci.* **264**, 507–525 (1966).
16. Gerlach, T. M. *Eos* **72**, 249–255 (1991).
17. Berner, R. A. *Am. J. Sci.* **282**, 451–473 (1982).
18. Romankevich, E. A. *Geochemistry of Organic Matter in the Ocean* (Springer, New York, 1984).
19. Burton, J. D. in *SCOPE 21: The Major Biogeochemical Cycles and their Interactions* (eds Bolin, B. & Cook, R. B.) 408–410 ((Wiley, New York, 1983).
20. Buat-Menard, P., Riley, J. P., Chester, R. & Duce, R. A. in *Chemical Oceanography*, vol. 10 (eds Riley, J. P., Chester, R. & Duce, R. A.) 251–279 (Academic, London, 1989).
21. Broecker, W. S. & Peng, T.-H. *Tracers in the Sea* (Eldigio, Palisades, New York, 1982).
22. Broecker, W. S. & Peng, T.-H. *Nature* **356**, 587–589 (1992).
23. Berner, R. A., Lasaga, A. C. & Garrels, R. M. *Am. J. Sci.* **283**, 641–683 (1983).
24. Berner, E. K. & Berner, R. A. *The Global Water Cycle* (Prentice-Hall, Englewood Cliffs, 1987).
25. Meybeck, M. *Am. J. Sci.* **287**, 401–428 (1987).
26. Drever, J. I., Li, Y.-H. & Maynard, J. B. in *Chemical Cycles in the Evolution of the Earth* (eds Gregor, C. B. *et al.*) 17–53 (Wiley, New York, 1988).
27. Schlesinger, W. H. & Melack, J. M. *Tellus* **33**, 172–187 (1981).
28. Meybeck, M. *Flux of Organic Carbon by Rivers to the Oceans* 219–269 (National Technical Information Service, Springfield, Virginia, 1981).
29. Milliman, J. D., Xie Quinchun & Yang Zuosheng *Am. J. Sci.* **284**, 824–834 (1984).
30. Ittekkot, V. *Nature* **332**, 436–438 (1988).
31. Meybeck, M. *Physical and Chemical Weathering in Geochemical Cycles* 247–272 (Kluwer, Dordrecht, 1988).
32. Spitzy, A. & Leenheer, J. in *SCOPE: Biogeochemistry of Major World Rivers* (eds Degens, E. T., Kempe, S. & Richey, J. E.) 213–232 (Wiley, New York, 1991).
33. Degens, E. T., Kempe, S. & Richey, J. E. in *SCOPE 42: Biogeochemistry of Major World Rivers* (eds Degens, E. T., Kempe, S. & Richey, J. E.) 323–347 (Wiley, New York, 1991).

ACKNOWLEDGEMENTS. We thank U. Siegenthaler for discussions, P. Rayner and J. R. Toggweiler for reviews, and J. Olszewski for help in preparing the manuscript. Support for J.L.S. was provided by the Carbon Dioxide Research Division of the Department of Energy, and by the Geophysical Fluid Dynamics Laboratory of the NOAA through the generosity of K. Bryan and J. Mahlman. E.T.S.'s contribution was supported under the United States Geological Survey Global Change Hydrology Program.

Seismological evidence for metastable olivine inside a subducting slab

Takashi Iidaka* & Daisuke Suetsugu†‡

* Earthquake Research Institute, University of Tokyo, Yayoi 1-1-1, Bunkyo-ku, Tokyo, 113, Japan
† Department of Earth and Planetary Physics, Faculty of Science, University of Tokyo, Yayoi 2-11-16, Bunkyo-ku, Tokyo, 113, Japan

THE nature and location of the olivine–spinel phase transition inside subducting slabs differ greatly from the situation in the surrounding mantle, due to the different temperature distribution inside the slabs. Two models have been proposed for this phase transition: one in which the location of the phase boundary between olivine and modified (β-phase) spinel is determined by equilibrium thermodynamics[1], and the other including a metastable olivine phase which persists to a depth of ~550 km (ref. 2). The location of the olivine–spinel transition in the slab may be relevant to the generation of deep earthquakes[3–5], and to the buoyancy forces driving subduction[6]. Here we use travel-time residuals from deep earthquakes recorded by the dense seismograph network in Japan to investigate the configuration of the olivine–spinel phase boundary inside the subducting Pacific plate. Theoretical travel-time residuals for the equilibrium model do not fit the observed residuals, whereas those for the metastable model do, implying the presence of metastable olivine inside the subducting slab.

The seismic discontinuity near 400 km depth (now generally referenced to as the '410-km discontinuity') is generally interpreted as the result of the phase change from olivine to β-spinel[7,8]. Thermodynamic data for the dependence of this phase change on pressure and temperature predict that the equilibrium phase boundary inside a cold downgoing slab will be distorted upwards because of the positive Clapeyron slope of the phase change[1,9]. On the other hand, under non-equilibrium conditions, metastable olivine may exist inside a cold slab at depths of 400 km or greater[2,10].

The question of whether metastable olivine exists in downgoing slabs has important geophysical implications. Recent mineralogical experiments suggest that the occurrence of deep earthquakes may be related to a phase change of metastable olivine[3–5] to a high-pressure phase. The existence of metastable olivine would also affect the driving force of the downgoing slab, because the large density difference between the metastable olivine and the β or γ phases of the surrounding mantle would influence the buoyancy force acting on the slab[6].

Here we analyse seismic travel-time data to determine whether metastable olivine exists in a downgoing slab. This has previously been attempted for the Tonga and Izu-Bonin slabs[11,12], but large errors in locating the hypocentre, due to sparse data, precluded a definitive conclusion.

We search for metastable olivine in the Pacific slab beneath southwestern Japan using travel-time data from deep events which took place beneath this region. We calculate theoretical travel-time residuals for two models. In the first[9] (called the equilibrium model hereafter) the olivine–β-phase boundary in the slab follows equilibrium thermodynamics; in the second[2,10] (called the metastable model hereafter) olivine persists metastably in the downgoing slab to a depth of 550 km. The equilibrium model is based on work by Schubert *et al.*[9] and the metastable model is based on work by Liu[10]. The dense seismic network in southwestern Japan minimizes the location errors of deep earthquakes beneath this region and enables us to investigate the detailed velocity structure in the slab.

We analyse P-wave arrival-time data from 29 events with depths ranging from 300 to 500 km beneath southwestern Japan and with magnitudes larger than 4.0. We use 63 seismograph stations from the seismic networks of the Earthquake Research Institute of the University of Tokyo and the National Research Institute for Earth Science and Disaster Prevention. These stations were chosen because they are located as close as possible to the up-dip direction of the slab (Fig. 1). The reading error

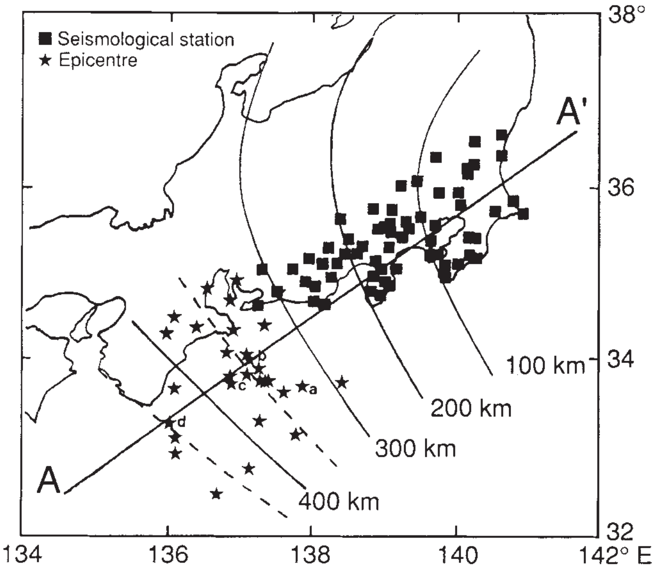

FIG. 1 Deep earthquake epicentres (stars) and seismic stations (squares). Iso-depth lines (in km) of the deep seismic zone are shown by solid contours. The points labelled a, b, c and d are the master events used for relocation of the hypocentres. Ray tracing along profile A–A′ is shown in Fig. 2.

‡ Present address: International Institute of Seismology and Earthquake Engineering, Building Research Institute, Tatehara, 1, Tsukuba, 305, Japan.